Supplemental Information:

Table S1: Best fit Gaussian means ± S.D. from fitting multi-spin distance distribution data to model III.

FliG site	FliM site	g-g' (Å)	m-m' (Å)	m-g (Å)	m-g' (Å)	g-m' (Å)
FliG 160 vs						
	FliM 60	45.5 ± 4.8	28.9 ± 4.2	39.2 ± 5.1	47.9± 4.9	
	FliM 167	45.5 ± 4.8	32.4 ± 4.3	44.8 ± 5.3	45 ± 5.1	
	FliM 121	45.5 ± 4.8	48 ± 4.2	20.2 ± 4.4	46.5 ± 4.1	49.2 ± 4.2
FliG 174 vs						
	FliM 60	43 ± 6.1	28.9 ± 4.2	31.8± 6.6	41.9 ± 4.25	48.1± 4.4
	FliG 305	46.2 ± 4.9	43± 6.1	30.4 ± 5.9	48.9 ± 5.4	

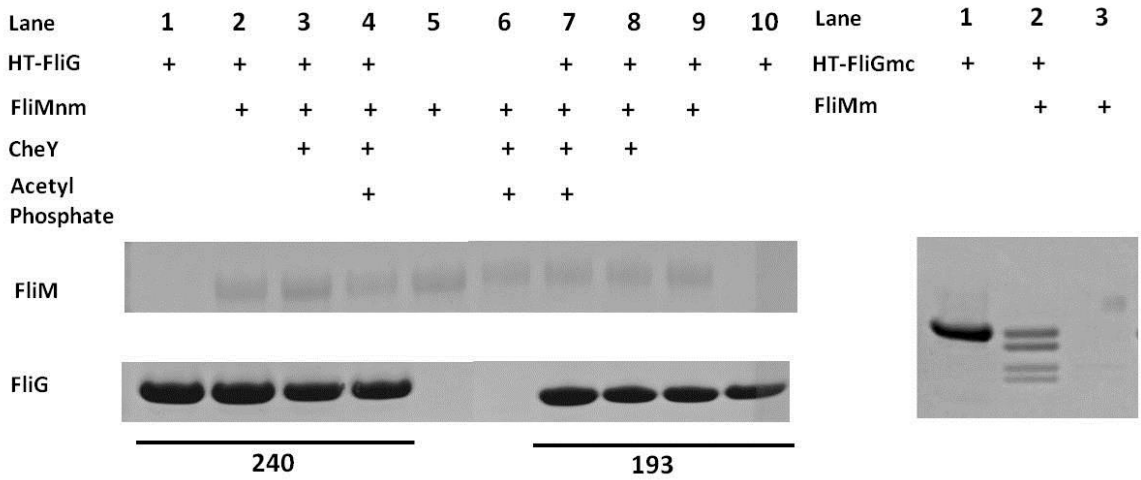

Figure S1. Interaction between FliM and $FliG_C$. Left: Pull-down assay of $FliM_{NM}$ with $FliG_C$ 240 (residues 240-335) (lanes 1-4) and $FliG_C$ 193 (residues 193-335) (lanes 7-10) in presence of CheY or CheY-P where indicated. Controls of $FliM_{NM}$ without tag (lane 5) in presence of CheY-P (lane 6) show some non specific binding to the affinity beads. No apparent binding is observed between $FliM_{NM}$ and $FliG_C$ (240 in lane 2 and 193 in lane 9) nor was it observed in presence of CheY (240 in lane 3 and 193 in lane 8) or CheY-P (240 in lane 4 and 193 in lane 7). Right: Positive control experiment showing the interaction between His_6-$FliG_{MC}$ (HT-$FliG_{MC}$) and $FliM_M$ (lane 2) performed under the same conditions as the samples on the left. Lanes 1 and 3 shows HT-$FliG_{MC}$ and $FliM_M$ respectively.

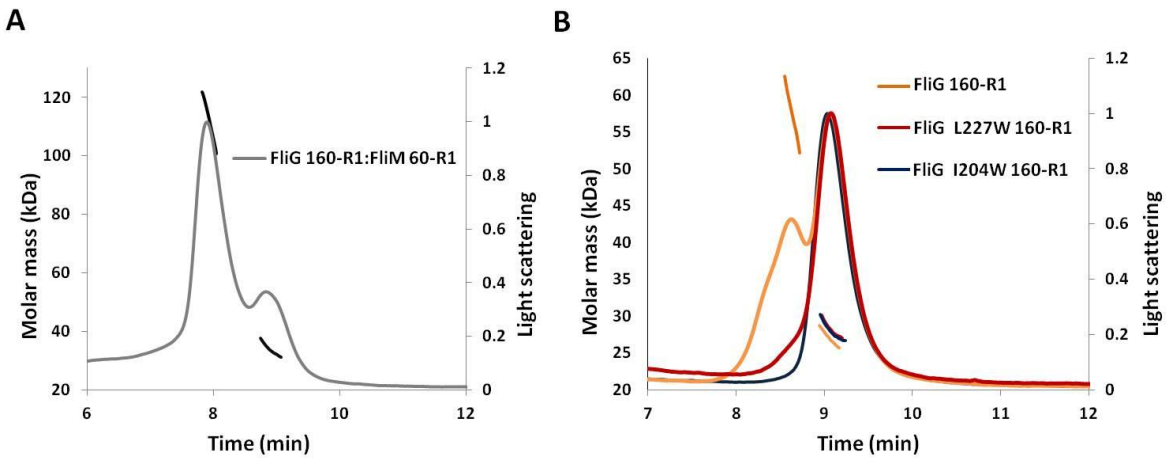

Figure S2. Multi-angle light scattering data on (A) FliG 160-R1:FliM 60-R1 showing formation of heterotetrameric complex (112 kDa) and excess FliM (33.7 kDa) under the conditions of the PDS experiment. Measurement with unlabelled protein also showed tetramer formation (data not shown) (B) FliG 160-R1 alone is a mixture of monomer (28.1 kDa) and dimer (57.3 kDa) whereas FliG L227W 160-R1 and FliG I204W 160-R1 behave as monomers (27.8 kDa and 27.1 kDa respectively). Unlabeled FliG also exists as a monomer in equilibrium with higher molecular weight species (data not shown).

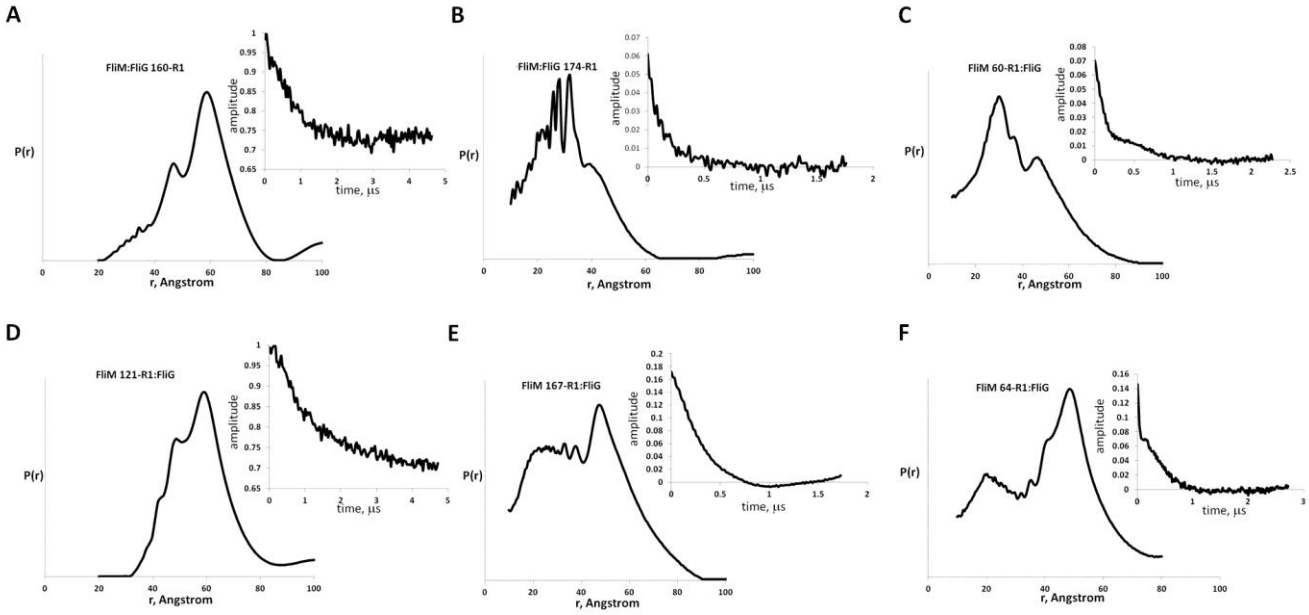

Figure S3. Distance distribution and time domain signal for spin label at (A) FliG 160-R1:FliM, (B) FliG 174-R1:FliM, (C) FliM 60-R1:FliG, (D) FliM 121-R1:FliG, (E) FliM 167-R1:FliG and (F) FliM64-R1:FliG. For (A) and (D), the measurement was performed in D_2O.

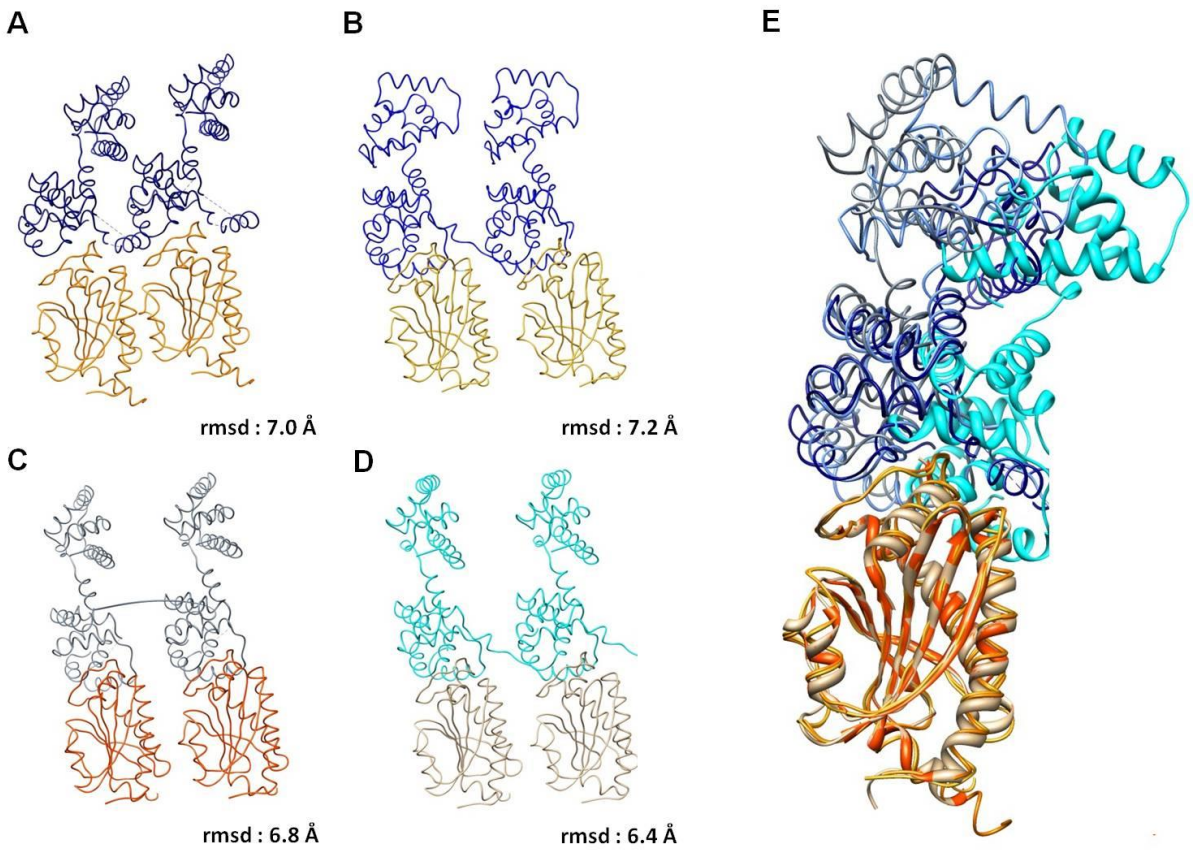

Figure S4. Different versions of model III used for fitting (A-D) with the corresponding rmsd with respect to the fit is indicated below. (E) Superposition of the FliM:FliG heterodimers from each version of model III tested (A-D).

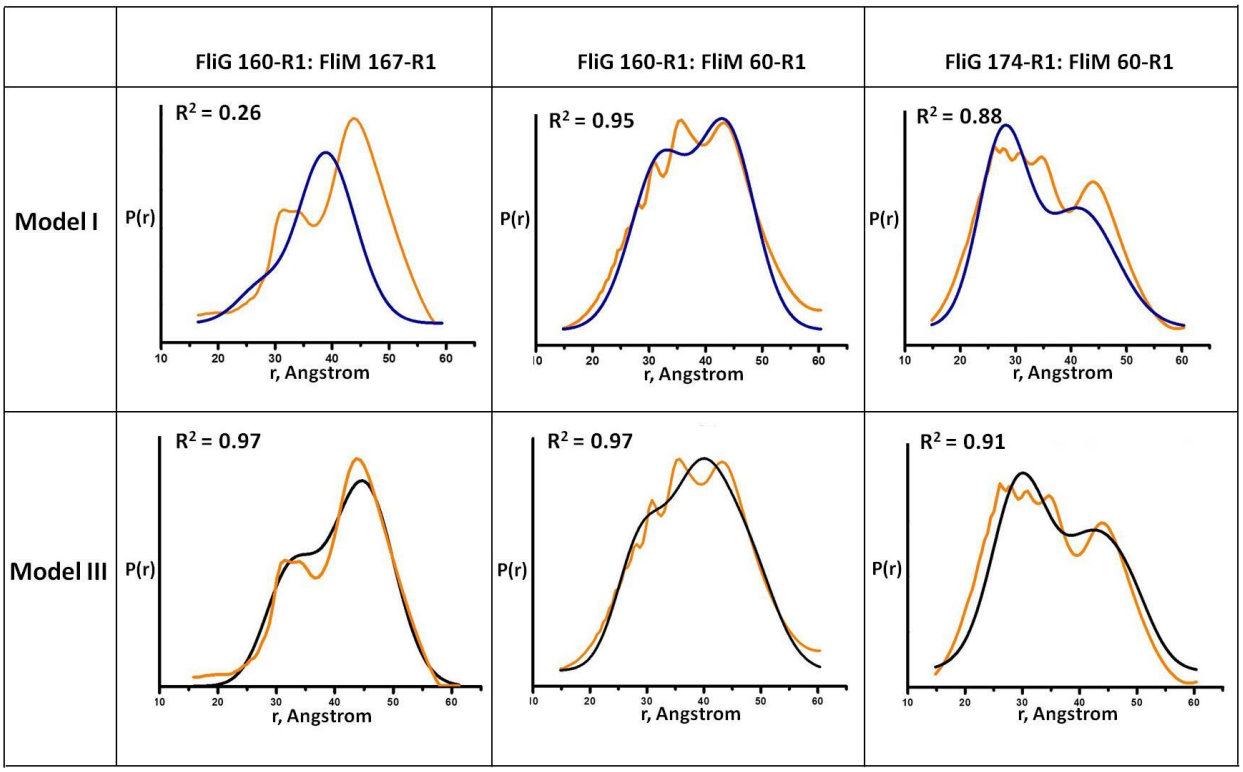

Figure S5. Qualitative analysis of distance distribution data using the antiparallel crystal structure (model I) for the fitting (top). Eqn 2 was used for fitting the anti-parallel arrangement of the FliM:FliG complex. Comparison of R^2 values and the envelope from the fitted Gaussian with the parallel model III (bottom) for each distribution indicates that model III act as a better model for the available data. In orange is the experimental distance distribution, blue curve is the sum of fitted Gaussian for model I and black curve is for model III.

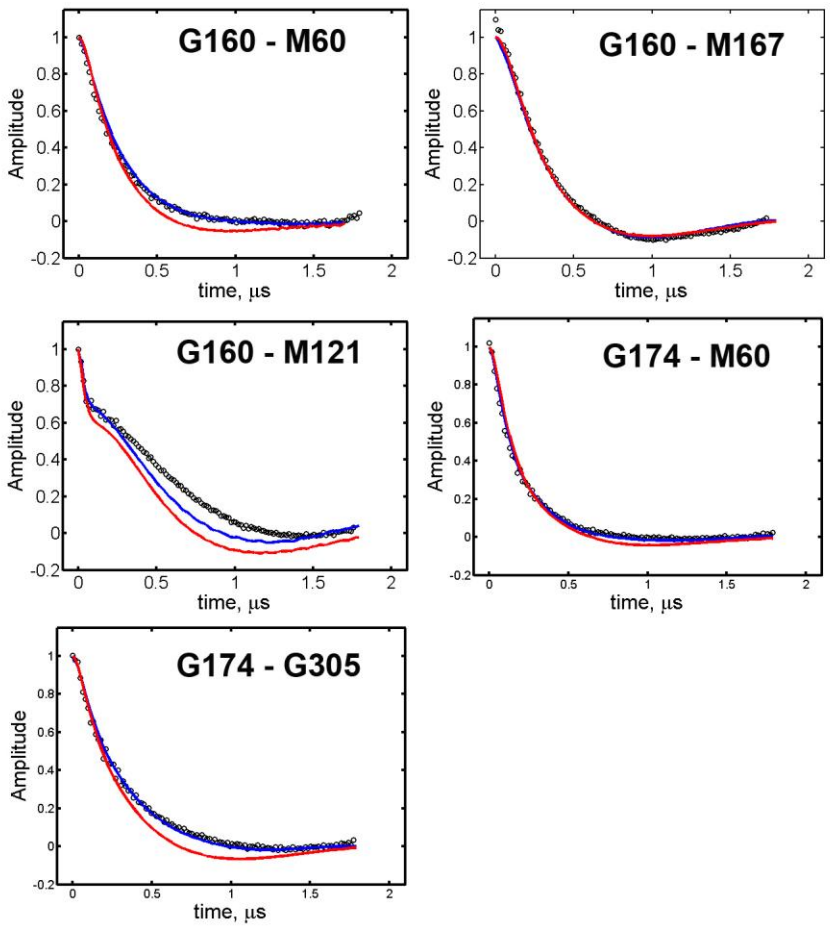

Figure S6. Reconstruction of DEER time-domain data from experimental P(r) distributions (blue) and Gaussian fits P(r) (red). Deviations from the experimental data (black) arise in part from inaccuracies in the time-domain baseline correction and the ability of the MEM treatment to filter minor features at long distances. Neither compensation to the original time domain data significantly changes the P(r) calculation.

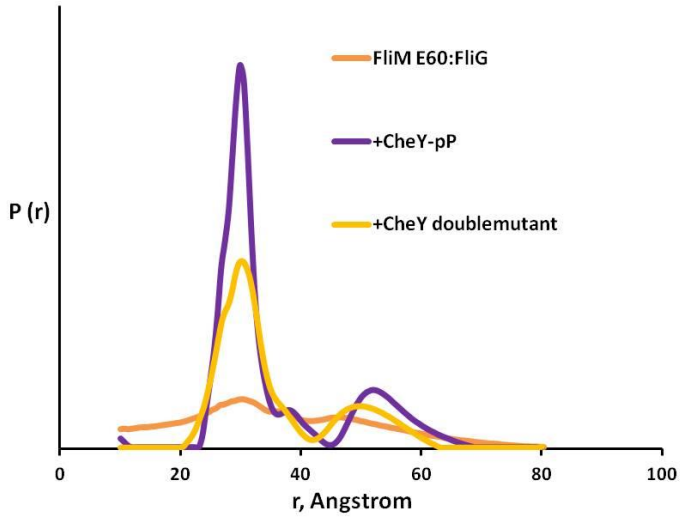

Figure S7. Changes in FliM spin distributions with activated CheY variants. Distance distributions for spin labels at FliM 60-R1:FliG (orange), with double mutant CheY(yellow), and with CheY-pP (purple).

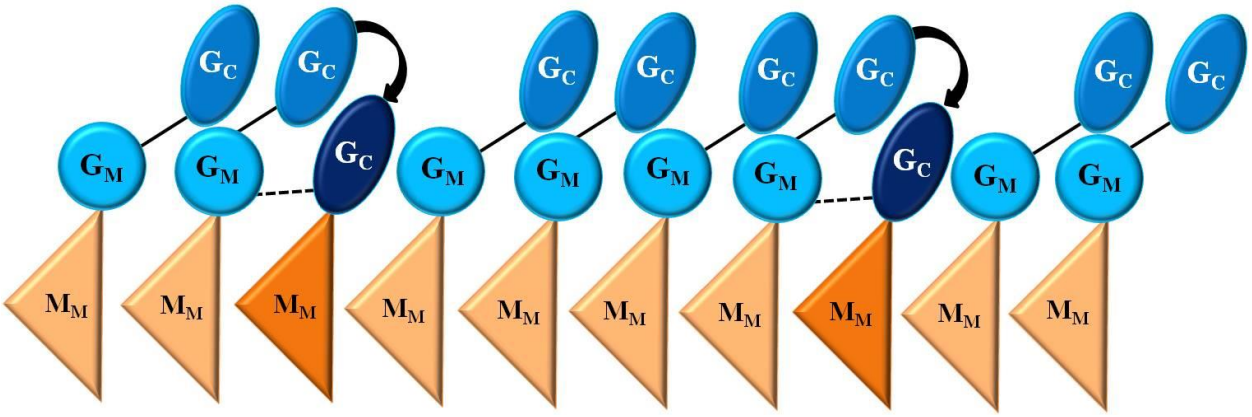

Figure S8. Possible arrangements of FliM and FliG based on the results from this study and the stoichiometry mismatch among the different rotor proteins. 26 copies of FliG interact with 26 copies of FliM (tan) through the middle domain. Gaps are created at the remaining 8 copies of FliM (dark orange) where no $FliG_M$ is present for binding. These 8 copies are likely randomly distributed in the C-ring. The C-terminal domains of a neighboring FliG (dark blue) may swing down and directly interact with $FliM_M$ through the conserved hydrophobic patch. This interaction between FliM and $FliG_C$ may only be observed in intact rotors.